



The Greenland Ice-Marginal Lake Inventory Series from 2016 to 2023

Penelope How¹, Dorte Petersen², Kristian K. Kjeldsen¹, Katrine Raundrup³, Nanna B. Karlsson¹, Alexandra Messerli², Anja Rutishauser¹, Jonathan L. Carrivick⁴, James M. Lea⁵, Robert S. Fausto¹, Andreas P. Ahlstrøm¹, and Signe B. Andersen¹

¹Department of Glaciology and Climate, Geological Survey of Denmark and Greenland, Denmark

²Department of Hydrology and Climate, Asiaq Greenland Survey, Greenland

³Department of Environment and Mineral Resources, Greenland Institute of Natural Resources, Greenland

⁴School of Geography and water@leeds, University of Leeds, UK

⁵Department of Geography and Planning, University of Liverpool, UK

Correspondence: Penelope How (pho@geus.dk)

Abstract. The Greenland Ice Sheet and its surrounding peripheral glaciers and ice caps are projected to be the largest cryospheric contributor to sea level rise in the next century. While glacial meltwater is typically assumed to flow directly into the ocean, ice-marginal lakes temporarily store a portion of this runoff, influencing glacier dynamics, lacustrine-driven ablation, ecosystems, and downstream hydrology. The size, abundance and dynamics of ice-marginal lakes are expected to change in the future. However, they remain under-represented in projections of sea level change and glacier mass loss. Here, we provide eight annual records across Greenland of lake abundance, lake surface extents, and surface water temperature estimates from 2016 to 2023. The dataset catalogs 2918 automatically classified ice-marginal lakes and reveals their evolving conditions over time. Our dataset fills critical gaps in understanding Greenland's terrestrial water storage and its implications for sea level change projections, providing a first step toward quantifying meltwater storage at ice margins. Equally important, it supports assessments of ice sheet and glacier dynamics, such as lacustrine-driven ablation, and Arctic ecological studies of lake changes impacting ecosystems. The inventory series will also aid environmental management and hydropower planning aligned with Greenland's proposed commitments under the Paris Agreement. The inventory series is openly accessible on the GEUS Data-verse (<https://doi.org/10.22008/FK2/MBKW9N>) with full metadata, documentation, and a reproducible processing workflow (How et al., 2025).

1 Introduction

The Greenland Ice Sheet and its peripheral glaciers and ice caps (PGICs) are forecast to be the largest cryospheric contributor to sea level rise over the coming century (Arctic Monitoring and Assessment Programme (AMAP), 2021). At present, these projections assume that meltwater from the Greenland Ice Sheet flows directly into the ocean, yet a portion of this is known to be stored temporarily in ice-marginal lakes, along the ice edge of the Greenland Ice Sheet and in front of and beside surrounding PGICs. The delayed release of meltwater at the ice margin is a significant, dynamic component of terrestrial storage. Ice-marginal lakes around the Greenland Ice Sheet form as meltwater becomes trapped at the terminus or edges of



an outlet glacier (How et al., 2021; Carrivick et al., 2022). Many of these lakes can be persistent and stable (Carrivick and Quincey, 2014), but an increasing number are recognised to be highly dynamic systems (Dømgaard et al., 2024). For example, many ice-marginal lakes in Greenland are prone to sudden and short-lived drainage events, thereby producing GLOFs (Glacial Lake Outburst Flood events) which are also referred to as *jökulhlaups* (Icelandic) or *sermimit supinerit* (direct translation into Kalaallisut, West Greenlandic; in singular *sermimit supineq*). GLOFs in Greenland can have characteristics of megafloods (Carrivick and Tweed, 2019) and have caused glacier speed-up events (e.g., Kjeldsen et al., 2017), influenced downstream erosion and sedimentation rates (e.g., Carrivick et al., 2013; Tomczyk et al., 2020), and water salinity (e.g., Grinsted et al., 2017; Kjeldsen et al., 2014).

The presence of an ice-marginal lake introduces a suite of thermo-mechanical processes, including lacustrine submarine melting and calving, that can dictate glacier margin morphology, dynamics and exacerbate ice mass loss (Sutherland et al., 2020; Carrivick and Tweed, 2019; Zhang et al., 2023b). At Russell Lake, situated beside Russell Glacier in Kangerlussuaq (West Greenland), these processes are relatively well-documented, illustrating how lake presence enhances melt-under-cutting and calving (Carrivick et al., 2017; Dømgaard et al., 2023). With continued retreat of the Greenland Ice Sheet under a warming climate, ice-marginal lakes and their associated processes are expected to become more abundant, larger, and warmer, which will likely amplify lacustrine-driven proglacial melt rates and GLOF events (Carrivick and Tweed, 2016; Grinsted et al., 2017; Shugar et al., 2020; Carrivick et al., 2022; Dye et al., 2021; Lützow et al., 2023; Rick et al., 2023; Veh et al., 2023; Holt et al., 2024; Zhang et al., 2024). However, ice-marginal lakes and their associated processes are largely absent from sea level change projections, which assume an immediate meltwater contribution to the ocean. This assumption overlooks the role of ice-marginal lakes as intermediary storage, and changes in lacustrine conditions, caused for instance when glaciers retreat onto land.

Mapping ice-marginal lakes is challenging due to the variability in lake characteristics. Remote sensing has been a viable approach for mapping the presence and surface extent of ice-marginal lakes, as demonstrated by inventories in Greenland (How et al., 2021), Alaska (Rick et al., 2022), Norway (Andreassen et al., 2022), Svalbard (Wieczorek et al., 2023) and High Mountain Asia (Chen et al., 2021). In general, classification approaches have been established to identify water bodies from SAR (Synthetic Aperture Radar) and multi-spectral (i.e. red, green, blue, near-infrared, shortwave) imagery, along with water potential identification using sink analysis from Digital Elevation Models (DEMs). As Greenland covers a large latitudinal range, ice-marginal lakes have very varying conditions which make them difficult to classify through one adopted method (How et al., 2021). For instance, surface sediment load, ice, and snow cover can vary significantly, with perennial ice cover in some cases at high latitudes and elevations (e.g., Mallalieu et al., 2021). Accordingly, multi-method classification approaches are necessary to capture this diversity (How et al., 2021).

Existing ice-marginal lake inventories are often static and therefore do not capture the dynamic nature of these lakes, nor capture new lakes and retire detached lakes once the margin has retreated. Given that ice-marginal lakes are projected to increase in size and abundance over time (Shugar et al., 2020; Zhang et al., 2024), it is of utmost importance to generate time-series that adequately capture ice-marginal lake change and assess the impact of these changes on future sea level projections.



Here, we present an annual series of Greenland ice-marginal lakes from 2016 to 2023, classified using an established multi-method remote sensing approach. Each annual inventory maps the number of lakes (i.e. abundance) and lake surface area, along with attributes such as known lake name and surface water temperature estimations. These inventories reveal evolving lake conditions that support future assessments of sea level contribution, ecosystem productivity, and biological activity associated with the Greenland Ice Sheet and the PGICs.

2 Data description

2.1 Dataset overview

The annual inventory series is a follow-on from the 2017 Greenland ice-marginal lake inventory, largely adopting the same classification approach, data structure and formatting (How et al., 2021). The dataset consists of a series of annual inventories, mapping the presence and extent of ice-contact lakes across Greenland (Figure 1). Ice-contact lakes are defined as water bodies > 0.05 km² (based on satellite image spatial resolution), which are immediately adjacent to the Greenland Ice Sheet and/or the PGICs of Greenland. The annual inventory series spans the entirety of Greenland, including all terrestrial regions. Thus far, there are 8 annual inventories, covering 2016 to 2023, where one inventory represents one year.

2.2 Data sources and acquisition

Ice-marginal lakes are identified using three established classification methods, from Synthetic Aperture Radar (SAR) and multi-spectral imagery, and Digital Elevation Models (DEMs). Classifications from SAR and multi-spectral imagery for each inventory year are identified from all available Sentinel-1 and Sentinel-2 image acquisitions for the months of July and August (Table 1). DEM classifications are made from a static data product which covers the period 2008 to 2016. Metadata for each identified lake includes a lake surface temperature estimate, which is derived from Landsat 8/9 thermal band imagery (Table 1).

2.3 Data format and structure

The inventory series data are distributed as polygon vector features in an open GeoPackage format (.gpkg), with coordinates provided in the WGS NSIDC Sea Ice Polar Stereographic North (EPSG:3413) projected coordinate system. File names follow the convention defined in the original 2017 Greenland ice-marginal lake inventory (Wiesmann et al., 2021; How et al., 2021):

`<inventory-year>-<funder>-<project-acronym>-IML-f<version-number>.<file-extension>.`

Each GeoPackage file contains metadata regarding the lake description, physical measurements, lake surface temperature, method/s of classification, verification and possible editing (Table 2). A key piece of metadata to highlight is the lake identification number ("lake_id", Table 2), which are assigned to each classified ice-marginal lake, often consisting of multiple polygon features and/or classifications. These unique identifications are compatible across inventory years, therefore supporting time-series analysis and comparison across inventories.



Table 1. Summary of satellite data sources

Satellite	Data product	Acquisition filters	Spatial resolution
Sentinel-1	Ground Range Detected (GRD) dual-polarization C-band SAR images	Interferometric Wide Swath (IW), Horizontal-Horizontal (HH) polarisation, 01 Jul to 31 Aug	10 metres
Sentinel-2	Multispectral instrument (MSI), Top of Atmosphere (TOA), Level 1C images	01 Jul to 31 Aug, 20% max. cloud cover	10 metres
-	ArcticDEM mosaic (version 3)	-	2 metres
Landsat 8/9	Operational Land Imager/Thermal Infrared Sensor (OLI/TIRS), Collection 2, Level 2, surface temperature science product	01 to 31 Aug, 30% max. cloud cover	30 metres

Information is included regarding whether the adjacent ice margin is either the ice sheet or PGIC ("margin", Table 2). This margin information originates from the MEaSUREs GIMP 15 m ice mask, previously used for the spatial filtering. In addition, each ice-marginal lake is assigned a region – north-west (NW), north (NO), north-east (NE), central-east (CE), south-east (SE), south-west (SW), and central-west (CW) ("region", Table 2). These regions and their corresponding names are based on ice sheet catchment regions from Mouginot and Rignot (2019), which are used to also extend to the terrestrial periphery beyond the ice sheet. By doing so, regional trends can be identified from ice-marginal lakes with a PGIC margin as well as the ice sheet (Carrivick et al., 2022).

Lake names ("lake_name", Table 2) are assigned in instances where a name is available, with preference to West Greenlandic (Kalaallisut) placenames followed by Old Greenlandic and alternative foreign placenames. Placenames are provided by Oqaasileriffik (the Language Secretariat of Greenland) placename database (<https://nunataqqi.gl/>), filtering placenames to those associated with lake features. The placename database is distributed with QGreenland v3.0 (Moon et al., 2023).

A readme file is included with the dataset that outlines the data file contents and terms of use. An additional data file is included which is a point vector GeoPackage file representing all identified lakes across the inventory series (presented in Figure 1). This includes manually identified lake locations that are not captured in the inventory series using the automated classification approaches.



Table 2. Summary of metadata included with each ice-marginal lake inventory in the annual series

Variable name	Description	Format
lake_id	Identifying number for each unique lake	Integer
lake_name	Lake placename, as defined by the placename database provided by Oqaasileriffik (the Language Secretariat of Greenland) (https://nunataqqi.gl/) which is distributed with QGreenland (https://qgreenland.org/). If no lake name is given then the placename is classed as "Unknown".	String
margin	Type of margin that the lake is adjacent to ("ICE_SHEET", "ICE_CAP")	String
region	Region that lake is located, as defined by Mouginot and Rignot (2019) ("NW", "NO", "NE", "CE", "SE", "SW", "CW")	String
area_sqkm	Areal extent of polygon/s in square kilometres	Float
length_km	Length of polygon/s perimeter in kilometres	Float
temp_aver	Average lake surface temperature estimate for the month of August (in degrees Celsius), derived from the Landsat 8/9 OLI/TIRS Collection 2 Level 2 surface temperature data product	Float
temp_min	Minimum pixel lake surface temperature estimate for the month of August (in degrees Celsius), derived from the Landsat 8/9 OLI/TIRS Collection 2 Level 2 surface temperature data product	Float
temp_max	Maximum pixel lake surface temperature estimate for the month of August (in degrees Celsius), derived from the Landsat 8/9 OLI/TIRS Collection 2 Level 2 surface temperature data product	Float
temp_stdev	Average lake surface temperature estimate standard deviation for the month of August, derived from the Landsat 8/9 OLI/TIRS Collection 2 Level 2 surface temperature data product	Float
temp_count	Number of Landsat 8/9 OLI/TIRS Collection 2 Level 2 scenes that lake surface temperature information were derived from. Scenes are only selected from the month of August	Integer
method	Method of classification ("DEM", "SAR", "VIS")	String
source	Image source of classification ("ARCTICDEM", "S1", "S2")	String
all_src	List of all sources that successfully classified the lake (i.e. all classifications with the same "lake_name" value)	String
num_src	Number of sources that successfully classified the lake ("1", "2", "3")	Integer
certainty	Certainty of classification, which is calculated from "all_src" as a score between "0" and "1"	Float
start_date	Start date for classification image filtering	String
end_date	End date for classification image filtering	String
verified	Flag to denote if the lake has been manually verified ("Yes", "No")	String
verif_by	Author of verification	String
edited	Flag to denote if polygon has been manually edited ("Yes", "No")	String
edited_by	Author of manual editing	String



3 Methodology

3.1 Lake classification

Lake classifications are based on those adopted in the production of the 2017 Greenland ice-marginal lake inventory, which is summarised in Figure 2 (How et al., 2021). The main progression (and therefore difference) is that the processing pipeline is now unified and operates through Google Earth Engine to conduct the heavy image processing (How, 2024), and filtering/post-processing conducted with open-source spatial packages in Python, namely geopandas (Kelsey et al., 2020) and rasterio (Gillies et al., 2013–). The Python pipeline is deployable as a package called GrIML (How, 2024), which is accompanied by thorough documentation and guidelines (<https://griml.readthedocs.io>). This ensures a high level of reproducibility and transparency that adheres to the FAIR (Findability, Accessibility, Interoperability, and Reusability) principles (Wilkinson et al., 2016).

110 3.1.1 SAR backscatter classification

Water bodies are classified from Sentinel-1 GRD scenes, which are dual-polarization C-band SAR images (Table 1). Scenes are pre-processed using the Sentinel-1 Toolbox to generate calibrated, ortho-corrected data, specifically thermal noise removal, radiometric calibration and terrain correction using either the SRTM 30 or ASTER DEM. Scenes are then filtered to IW swath and HH polarisation, with image acquisitions limited to the summer months (1 July to 31 August) of each inventory year (2016 to 2023). Averaged mosaics for each year are derived from all summer scenes for each year of the inventory series at a 10 m spatial resolution. These mosaics are smoothed using a focal median of 50 metres. Classifications are derived from these averaged and smoothed mosaics using a static threshold trained for detecting open water bodies (How et al., 2021).

3.1.2 Multi-spectral indices classification

Water bodies are classified from Sentinel-2 MSI, TOA, Level-1C scenes acquired for the summer months (1 July to 31 August) of each inventory year (2016 to 2023) (Table 1). Clouds are masked using the cloud mask provided with each scene (QA60), masking out opaque and cirrus clouds. The bands of interest are extracted, specifically blue (B2), green (B3), red (B4), near-infrared (B8), and the two shortwave infrared bands (B11, B12) (Table 3). The shortwave infrared bands are resampled from 60 m to 10 m spatial resolution, and then averaged band mosaics are produced from all summer scenes for each inventory year.

Five spectral indices are used to classify open water bodies: 1) Normalised Difference Water Index (McFeeters, 1996); 2) Modified Normalised Difference Water Index (Xu, 2006); 3) Automated Water Extraction Index (with shadow) (Feyisa et al., 2014); 4) Automated Water Extraction Index (no shadow) (Feyisa et al., 2014); 5) Snow brightness ratio (How et al., 2021) (Table 3). The thresholds for the indices are chosen based on previous studies of ice-marginal lakes (How et al., 2021; Shugar et al., 2020), where positive classifications adhere to all thresholds.



Table 3. Summary of multi-spectral indices for ice-marginal lake classification from Sentinel-2 Level 1C scenes

Spectral index	Equation	Threshold/s	Target
Normalised Difference Water Index (NDWI)	$(B3 - B8) \div (B3 + B8)$	< 0.3	Open water with shadowing
Modified Normalised Difference Index (MNDWI)	$(B3 - B11) \div (B3 + B11)$	> 0.1	Snow/ice in water
Automated Water Extraction Index (with shadow) (AWEIsh)	$B2 + 2.5 \times B3 - 1.5 \times (B8 + B11) - 0.25 \times B12$	> 2000 & < 5000	Optimised sediment-loaded water without shadowing
Automated Water Extraction Index (no shadow) (AWEInsh)	$4 \times (B3 - B11) - (0.25 \times B8 + 2.75 \times B12)$	> 4000 & < 6000	Sediment-loaded water with shadowing
Snow Brightness Ratio (BRIGHTNESS)	$(B4 + B3 + B2) \div 3$	< 5000	Snow-covered areas

3.1.3 Sink classification

130 Water bodies are classified from the ArcticDEM 2-metre mosaic (version 3), which is compiled from the best quality Arctic-
 DEM strip files and manually adjusted to form a static data product (Table 1). The mosaic is smoothed using a focal median
 of 110 metres, and DEM depressions (i.e. where water pools) are filled over a 50-pixel moving window and subsequently sub-
 135 tracted from the original mosaic; producing the outline of a lake. It is noted that this is an indirect water classification method
 compared to the former two approaches (which directly detect water). Therefore, validation is required to confirm the presence
 of water in classified DEM sinks, which will be elaborated further in the following subsection.

3.2 Summer surface water temperature estimation

A summer surface water temperature estimate is provided with each classified lake across inventory years. Surface water tem-
 perature estimates are derived from the Landsat 8 and Landsat 9 OLI/TIRS surface temperature data, which is a Collection 2,
 Level-2 science product that is part of a large Landsat re-processing effort (Table 1). Surface temperature estimates are gener-
 140 ated from descending, day-lit Landsat 8/9 acquisitions with thermal infrared band information (30 metre spatial resolution) and
 auxiliary data (i.e. Top Of Atmosphere reflectance and brightness temperature), along with ASTER datasets (global emissivity
 and normalised difference vegetation index) and atmospheric data (geopotential height, specific humidity and air temperature)
 (Earth Resources Observation and Science (EROS) Center, 2020; Malakar et al., 2018).



Due to the lack of in situ lake surface temperature measurements in Greenland, the scheme proposed by Dyba et al. (2022) is adopted, whereby surface temperature values (LST_{land}) are corrected to surface water temperature (LST_{water}) using the following calibration:

$$LST_{scaled} = LST_{land} \times 0.00341802 + 149.0 \quad (1)$$

$$LST_{water} = (0.806 \times LST_{scaled} + 54.37) - 273.15 \quad (2)$$

Where LST_{scaled} is the applied scale factor for computing temperature in Kelvin (K) units, and LST_{water} is the calibrated surface water temperature in degrees Celsius (NASA Applied Remote Sensing Training (ARSET) program, 2022; Dyba et al., 2022). This calibration has previously shown strong correlations against in situ measurements (average RMSE = 2.8 °C and $R^2 = 0.8$) from 38 lakes in Poland, highlighting accurate estimates through a simple linear calibration (Dyba et al., 2022). Ideally, a correction factor specifically for calibrating values to Greenland lakes would be adopted. However, in situ validation datasets in Greenland are sparse and the derived correction factor appears to agree well with the limited datasets available. In the future, more in situ observations would strengthen the assessment, with a possibility to derive a Greenland specific correction scheme.

A summer average surface water temperature estimate is derived using this approach for each lake extent in the ice-marginal lake inventory series. Scenes are filtered by a maximum cloud cover of 20%, with acquisitions limited to the month of August to reduce the probability of ice-covered lake conditions. Lake extents are cropped by a border pixel (i.e. 30 metres) to reduce the impact of edge effects. An average, maximum and minimum surface water temperature value is computed for each lake extent over each inventory year, along with the standard deviation.

4 Results

4.1 Lake abundance

The dataset identifies 2918 automatically delineated ice-marginal lakes (Figure 1). Of these lakes, 2054 share a margin with the ice sheet whilst 864 are in contact with PGICs (Figure 3). The SW region holds the most lakes compared to other regions, with 786 classifications (640 classified at the ice sheet margin and 146 at the PGIC margins). A high abundance of PGIC lakes is found in the NO region, with 278 lakes, compared to only 37 PGIC lakes in SE. This reflects the presence of more PGICs in northern Greenland, compared to the greater ice sheet cover in the southeast.

Small fluctuations in the abundance of lakes are evident, fluctuating between 1963 (inventory year 2021) and 1827 (inventory year 2022) lakes (Figure 3). The largest variation in lake abundance at the ice sheet is evident at the SW margin, with a fluctuating range of 48 lakes (8%) between 567 (2018, 2023) and 615 lakes (2021) (Figure 3a). The CW and SE margin experienced the least variability, only varying by 16 lakes and 15 lakes, respectively. Changes in lake abundance at the ice sheet margin do not follow any spatial or temporal trends, with fluctuations unconnected to inventory year or margin region.

Lakes at the margins of periphery ice caps and glaciers vary between 723 (inventory year 2022) and 806 (inventory year 2019), with an average range of 11 lakes at the margins of periphery ice caps and glaciers (compared to an average range of 26 lakes at the ice sheet margin) (Figure 3b). The largest fluctuations in lake abundance are seen in the NO and NE regions,



fluctuating by 22 (8%) and 29 lakes (14%), respectively. This is linked to the higher number of lakes in these regions, which is supported by the smallest fluctuations evident in the regions where fewer lakes are present (i.e. NW, SE, CE and CW).

4.2 Lake surface extent

The largest lake in the inventory is Romer Sø, located in northeast Greenland, with a total area of 126.86 km² (Figure 1). The average lake size is 1.29 km², and the median lake size is 0.27 km² with 2395 lakes between 0.05-1.00 km² (82%). Only 59 lakes in the inventory series have a total area above 10 km² (2%). The NE and SW regions hold the largest lakes on average, with an average lake area of 1.63 km² (median: 0.34 km²) and 1.58 km² (median: 0.27 km²), respectively. On average, the largest PGIC lakes are also located in the NE region (1.43 km²), likely because Romer Sø skews the PGIC average for this region.

The inventory series also holds information on the change in lake area over time, by comparing corresponding lake extents from each inventory year classified using a direct classification method (i.e. from SAR and/or multi-spectral imagery) (Figure 3). Change in average lake area over the ice sheet margin is relatively consistent across the inventory series, with the smallest change evident at the CE ice sheet margin (0.30 km²) and the largest change evident at the NO ice sheet margin (1.31 km²) (Figure 3a). Average lake size is highest in the NE region in 2022, with an average size of 2.77 km², coinciding with the lowest lake abundance (448). The average lake area is smaller across Greenland's PGIC margins, with an average lake area of 1.00 km², compared to lakes adjacent to the ice sheet with an average lake area of 1.40 km². Fluctuations in the average lake area across the inventory series are generally much smaller, apart from in the CE and NE regions which range across 2.20 km² and 1.76 km², respectively (Figure 3b).

Overall, lake area change trends can be tracked at 918 lakes in the inventory series (31% of all mapped lakes), with 243 experiencing growth between 2016 and 2023 (i.e. an increase in area of > 0.05 km²), 675 declining in size (i.e. a decrease in area of > 0.05 km²) and 778 remaining the same size (i.e. a change in lake area limited to \pm 0.05 km²) (Figure 4). The largest lake area changes are experienced at the larger lakes generally, such as those found in the NE region (Figure 4b) and the SW region (Figure 4d).

The inventory series demonstrates changes to lake morphology (and the corresponding change in ice margin morphology), of which four example scenarios are presented in Figure 5. A classic terminus basin retreat style is evident across many ice-marginal lake extents, as presented in Figure 5a, where terminus retreat/lake expansion is marked in the central section of the glacier outlet, leaving a trailing terminus morphology at the lateral margins. Peripheral terminus retreat is highlighted in Figure 5b, where terminus retreat/lake expansion is focused at the lateral margins. There are instances where the presence of a lake affects the boundary conditions of two glacier termini, as demonstrated in Figure 5c, where two glaciers terminate into the same common ice-marginal lake. And finally, there are instances displayed in the inventory series where there is margin retreat/lake expansion focused around a discrete zone, such as in Figure 5d where a marked embayment has formed at a particular point in the north region of the glacier terminus.



4.3 Lake surface temperature

210 An average surface temperature estimate is derived for each inventory lake from all available Landsat 8/9 scenes acquired in the month of August for each inventory year (see Section 3.2). This information is provided in the metadata of the ice-marginal lake inventory series. The average lake surface temperature fluctuates between 4.3 °C (2018) and 5.9 °C (2023) (Figure 6). Fluctuations year on year vary, with instances of lake temperature falling between annual time steps (e.g. from 5.7 °C to 5.5 °C from 2019 to 2020), rising (e.g. from 5.5 °C to 5.9 °C from 2022 to 2023), and remaining consistent (e.g. between 5.4 °C and 5.5 °C from 2020 to 2022).

215 5 Data quality and validation

5.1 Data quality control

Identified water bodies are compiled for each inventory year and filtered via three strategies: 1) by location; 2) by size; 3) by manual curation (Figure 2). Firstly, lakes are filtered based on their location relative to the ice margin. Here, a 1 km buffer is derived around the MEaSURES GIMP 15 m ice mask and classified water bodies are retained if they are located within the 220 buffer (Howat, 2017; Howat et al., 2014). Classified water bodies are filtered by size, only retaining lakes above a minimum size threshold of 0.05 km² based on the spatial resolution of the source satellite imagery; as adopted by How et al. (2021). Finally, each inventory year dataset is manually curated to remove misclassifications, edit classifications (for example, where the shadowing mask does not adequately remove shadowing effects), remove detected water bodies that do not hold water in specific years, and remove water bodies that are detached from the ice margin. This manual curation is carried out via visual 225 inspection of Sentinel-2 TOA Level-1C true colour composites from each inventory year.

Classification information is provided with the ice-marginal lake inventory series, so that the performance of each classification method can be evaluated (Figure 7). 14,020 of all detections in the inventory series (66%) are classified using only one of the methods, composed largely from the DEM method (Figure 7a). 5156 detections are classified using two methods (24%), and 2264 detections are classified using all three methods (11%). It is noted that the number of classification methods is not 230 a measure of certainty but instead should be interpreted as a reflection of lake appearance and its adherence to the criteria of each classification method, as well as satellite data availability.

The SW region is typically where most lakes were classified with all three classification methods; across both the ice sheet margin (Figure 7b) and the PGIC margins (Figure 7c). This is likely because the classification methods have been extensively applied and developed in the SW region compared to others (e.g., Carrivick and Quincey, 2014; Carrivick et al., 2017; Kjeldsen 235 et al., 2017). The DEM method is heavily relied upon in the NO and NE regions where direct classification of open water is challenging as lakes are more likely to be consistently ice/snow covered, and satellite image availability from Sentinel-1 and Sentinel-2 can be limited (How et al., 2021).



5.2 Lake abundance error estimation

Previous error analysis suggested that the 2017 ice-marginal lake inventory captured 92% of lake abundance, based on comparison between the inventory and user-defined lakes over four regions at the NE, NW and SW ice sheet margin, and a region within the PGICs, covering a collective area of 40,000 km². This formed an error estimate for lake abundance of ± 8% (see How et al. (2021) for more details). As a follow-on to this effort, ice-marginal lakes are manually verified for each inventory year, including those that were not classified using the automated methods. Across all inventory years, 4543 ice-marginal lakes have been manually identified in total, of which 2915 (64%) are present in the ice-marginal lake inventory series. This forms a revised lake abundance error estimation of ± 809 (36%). This error estimation is substantially different from the former estimate because the 2017 ice-marginal lake inventory included manual lake delineations, whereas the inventory series presented here only includes automated classifications (i.e. no manual lake delineations are included).

5.3 Surface lake temperature error estimation

Surface water temperature estimates are validated against all known and/or open-access in situ measurements of lake temperature in Greenland (Figure 8). The only continuous/long-term in situ surface measurements (i.e. <= 2 m) are from six lake records in southwest Greenland - Kangerluarsunnguup Tasia (64°07'50"N, 51°21'36"W) and Qassi-Sø (64°09'14"N, 51°18'27"W) (Greenland Ecosystem Monitoring, 2024), Russell Lake (67°13'77"N, 50°07'63"W) (courtesy of Kristian K. Kjeldsen), and three lakes as part of the Asiaq Greenland Survey hydrological monitoring programme (Qassi-Sø 2024 measurements; Qamanersuaq, 63°47'71"N, 50°00'50"W; and an unnamed lake referred to as Asiaq station 924, 64°12'99"N, 51°36'39"W).

Comparison of the 133 coinciding in situ measurements with those estimated using the remote sensing approach adopted here exhibit a strong correlation ($r^2 = 0.87$), with an RMSE of 1.68 °C, suggesting that the remotely sensed temperature estimates are reliable (Figure 8). This trend appears to be consistent regardless of the time of year. An error estimation of ± 1.2 °C is determined, based on the average difference from data points across all lake sites.

260 6 Potential applications and future updates

6.1 Uses for the ice-marginal lake inventory series

The inventory series presented here is the first step to quantify the terrestrial storage of meltwater, and how it changes over time, which would be highly valuable for refining estimations of the future sea level contribution of the Greenland Ice Sheet and surrounding PGICs. The ice-marginal lake inventory series is applicable to climate and cryosphere research, enabling inter-annual comparison of lake change (abundance, extent and surface temperature) over time, similar to inventories for other regions such as Svalbard (Wieczorek et al., 2023). Such inventories have been used to characterise ice dam types (e.g., Rick et al., 2022), monitor GLOFs (e.g., Lützow et al., 2023), and assess lake conditions in catchments of interest (e.g., Hansen et al., In Press). Lake conditions could also provide insights into glacier dynamics in lacustrine settings around Greenland, for



example, to investigate submarine melting in lacustrine settings and its impact on glacier retreat (e.g., Mallalieu et al., 2021).
270 More widely, the lake changes documented in this inventory series would be valuable to studies of the redistribution of mass
on the earth surface, affecting gravity, geodesy and lithospheric elastic response (e.g., Ran et al., 2024).

Beyond scientific research, the inventory series will also be a useful resource in Greenland's assessment of infrastructure,
with hydropower being the main sector that could benefit. Given Greenland's commitment to the Paris Agreement strongly
suggests the expansion of current hydropower infrastructure, the ice-marginal lake inventory series could be valuable in infras-
275 tructure assessments (Naalakkersuisut, 2023). For example, the inventory series can be used to distinguish glacier-fed lakes
from catchment-fed lakes, identify draining lakes, and other characteristics that are useful to discern viable catchment regions.

6.2 The future of the ice-marginal lake inventory series

It is planned to update the ice-marginal lake inventory series annually with new inventory years, using the methodology and
data sources outlined here. A possibility could be to also include past years, prior to the Sentinel satellite era, however, this
280 is limited by the open availability of SAR and multi-spectral satellite imagery at a high spatial resolution (i.e. 10 metres).
Another avenue to explore is the inclusion of manually delineated lake extents where lakes have not been identified with the
automated classification approaches. However, this would add further labour to the manual curation of the inventory series. An
alternative would be to look at implementing new automated classification methods with machine learning, using the existing
lake classifications as the foundation of a training dataset. Lake classification aided by machine learning has been successfully
285 used for supraglacial lake detection on the Greenland Ice Sheet, so the use of machine learning in ice-marginal lake detection
is likely to be feasible (Lutz et al., 2023; Melling et al., 2024).

One of the key limitations of this work to be addressed in the future is the reliance on static data products, in particular the
static ArcticDEM 2 m mosaic for classification, and the MEaSURES GIMP static ice margin for filtering. The use of static
data products in the inventory series presented here highlights the importance of high-labour, time-consuming manual dataset
290 curation. For the DEM classification, an alternative would be the ArcticDEM strip data product, which is time variant, but data
coverage is lacking currently and scenes covering all Greenland are not possible from year to year. Another option would be to
use coarser spatial resolution DEM products, such as PRODEM (500 m) (Winstrup et al., 2024), however, smaller lakes would
not be identifiable. For the ice margin filtering, machine learning ice margin products show promise in being used in future
editions of the inventory series, such as AutoTerm (trained with the TeamPicks dataset) (Goliber et al., 2022; Zhang et al.,
295 2023a). The use of dynamic ice margin datasets in the future could negate the need for generating a classification spatial buffer
around the margin data and instead classify ice-marginal lakes directly from their intersection with the ice margin position.

Another opportunity to further the inventory series would be the addition of valuable metadata on the characteristics and
dynamics of each classified ice-marginal lake. The type of damming has been included in other inventories, proving to be
useful for assessing present and future lake conditions under a changing climate (e.g., Rick et al., 2022). Incorporating known
300 GLOFs and/or drainage periods for each lake would also provide insight into abrupt changes in terrestrial water storage and be
highly valuable information for infrastructure assessments, such as hydropower utilities (e.g., Dømsgaard et al., 2024).



7 Conclusions

Here, a series of annual inventories is presented that represent ice-marginal lake abundance, surface area extents, and surface temperature estimates across Greenland for the years 2016 to 2023. Ice-marginal lakes are mapped across the margin of the Greenland Ice Sheet and its surrounding PGICs. The dataset demonstrates lake change over the 8-year period, which can be assessed at various scales, from individual lake, to regional, to Greenland-wide change. The annual ice-marginal lake inventory series is openly available on the GEUS Dataverse with a cite-able DOI at <https://doi.org/10.22008/FK2/MBKW9N>, including supporting metadata and documentation (How et al., 2025).

With each year, a new addition will be added to this dataset, with the hope that the inventory series could be used in the future to assess lake change at multi-decadal time scales. This is supported by GrIML, an open processing workflow with open-source programming that is accessible to novice programmers with thorough documentation and straightforward deployment (How, 2024).

The annual ice-marginal lake inventory series is a valuable addition to addressing current limitations in terrestrial water storage and its influence on Greenland's future sea level contribution. This dataset is the first step towards quantifying meltwater storage at the margins of the Greenland Ice Sheet, and surrounding PGICs. It also provides insight into lake change over time, and the resulting impact on glacier dynamics, such as lacustrine frontal ablation (i.e. submarine melting and calving). Beyond the cryospheric science community, the dataset will be invaluable to related disciplines in biology and ecology, where changes in lake conditions shape Arctic ecosystems and biological activity. On a national level, the inventory series could be a useful resource in environmental management and infrastructure assessment, for instance in the expansion of hydropower utilities as suggested in Greenland's new commitments to the Paris Agreement.

8 Code and data availability

The dataset is openly available on the GEUS Dataverse at <https://doi.org/10.22008/FK2/MBKW9N> (How et al., 2025), distributed under a CC BY 4.0 license (<https://creativecommons.org/licenses/by/4.0/>). If the dataset is presented or used to support results of any kind then we ask that a reference to the dataset be included in publications, along with any relevant publications from the data production team. If the dataset is crucial to the main findings, we encourage users to reach out to the authorship team as this will likely improve the quality of the work that uses this product. The production code for making the inventory series is openly available at <https://github.com/GEUS-Glaciology-and-Climatology/GrIML> (How, 2024). It is distributed as a deployable and version-controlled Python package. If the production code is used or adapted, then we ask for a reference to be included in publications.

Author contributions. P.H. led the production workflow and dataset presented, with input from D.P., K.K.K., N.B.K., A.M., A.R., J.L.C. and J.M.L. Validation datasets were collected and curated by D.P., K.K.K. and K.R. Management of the project and work presented was overseen by R.S.F., A.P.A. and S.B.A. All authors contributed to the manuscript text.



Competing interests. The authors declare that there are no competing interests.

Acknowledgements. P.H. was supported by an ESA (European Space Agency) Living Planet Fellowship (4000136382/21/I-DT-Ir) entitled "Examining Greenland's Ice Marginal Lakes under a Changing Climate (GrIML)". Further support was provided by the Programme for Monitoring of the Greenland Ice Sheet (PROMICE), funded by the Geological Survey of Denmark and Greenland (GEUS) and the Danish Ministry of Climate, Energy and Utilities under the Danish Cooperation for Environment in the Arctic (DANCEA), conducted in collaboration with DTU Space (Technical University of Denmark) and Asiaq Greenland Survey. In situ lake temperature datasets are supported by the GrIML project (with measurement collection led by Asiaq Greenland Survey), BioBasis under the Greenland Ecosystem Monitoring Programme (GEM), and the Greenland Integrated Observing System (GIOS) under the Danish Agency for Higher Education and Science. K.K.K. acknowledges support from the Independent Research Fund in Denmark (grant ID 10.46540/3103-00234B). J.M.L. acknowledges support from his UK Research and Innovation (UKRI) Future Leaders Fellowship (MR/X02346X/1). Additional thanks to Stephen Plummer and Marcus Engdahl for technical advice and support, and Sikkersoq Olsen and Arnaq Brandt Johansen from Oqaasileriffik (the Language Secretariat of Greenland) for clarification on the Kalaallisut terminology for GLOFs.



345 References

- Andreassen, L. M., Nagy, T., Kjølmoen, B., and Leigh, J. R.: An inventory of Norway's glaciers and ice-marginal lakes from 2018–19 Sentinel-2 data, *Journal of Glaciology*, 68, 1085–1106, <https://doi.org/10.1017/jog.2022.20>, 2022.
- Arctic Monitoring and Assessment Programme (AMAP): Arctic Climate Change Update 2021: Key Trends and Impacts. Summary for Policy-makers, Arctic Monitoring and Assessment Programme (AMAP), Tromsø, Norway, 16 pp, 2021.
- 350 Carrivick, J. L. and Quincey, D. J.: Progressive increase in number and volume of ice-marginal lakes on the western margin of the Greenland Ice Sheet, *Global and Planetary Change*, 116, 156–163, 2014.
- Carrivick, J. L. and Tweed, F. S.: A global assessment of the societal impacts of glacier outburst floods, *Global and Planetary Change*, 144, 1–16, <https://doi.org/10.1016/j.gloplacha.2016.07.001>, 2016.
- Carrivick, J. L. and Tweed, F. S.: A review of glacier outburst floods in Iceland and Greenland with a megafloods perspective, *Earth-Science Reviews*, 196, 102876, <https://doi.org/10.1016/j.earscirev.2019.102876>, 2019.
- 355 Carrivick, J. L., Turner, A. G. D., Russell, A. J., Ingeman-Nielsen, T., and Yde, J. C.: Outburst flood evolution at Russell Glacier, western Greenland: effects of a bedrock channel cascade with intermediary lakes, *Quaternary Science Reviews*, 67, 39–58, <https://doi.org/10.1016/j.quascirev.2013.01.023>, 2013.
- Carrivick, J. L., Tweed, F. S., Ng, F., Quincey, D. J., Mallalieu, J., Ingeman-Nielsen, T., Mikkelsen, A. B., Palmer, S. J., Yde, J. C., Homer, R., Russell, A. J., and Hubbard, A.: Ice-Dammed Lake Drainage Evolution at Russell Glacier, West Greenland, *Frontiers in Earth Science*, 5, 100, <https://doi.org/10.3389/feart.2017.00100>, 2017.
- 360 Carrivick, J. L., How, P., Lea, J. M., Sutherland, J. L., Grimes, M., Tweed, F. S., Cornford, S., Quincey, D. J., and Mallalieu, J.: Ice-Marginal Proglacial Lakes Across Greenland: Present Status and a Possible Future, *Geophysical Research Letters*, 49, e2022GL099276, <https://doi.org/https://doi.org/10.1029/2022GL099276>, 2022.
- 365 Chen, F., Zhang, M., Guo, H., Allen, S., Kargel, J. S., Haritashya, U. K., and Watson, C.: Annual 30 m dataset for glacial lakes in High Mountain Asia from 2008 to 2017, *Earth System Science Data*, 13, 741–766, <https://doi.org/10.5194/essd-13-741-2021>, 2021.
- Dømggaard, M., Kjeldsen, K. K., Huiban, F., Carrivick, J. L., Khan, S. A., and Bjørk, A. A.: Recent changes in drainage route and outburst magnitude of the Russell Glacier ice-dammed lake, West Greenland, *The Cryosphere*, 17, 1373–1387, <https://doi.org/10.5194/tc-17-1373-2023>, 2023.
- 370 Dømggaard, M., Kjeldsen, K., How, P., and Bjørk, A.: Altimetry-based ice-marginal lake water level changes in Greenland, *Communications Earth and Environment*, 5, 365, <https://doi.org/10.1038/s43247-024-01522-4>, 2024.
- Dyba, K., Ermida, S., Ptak, M., Piekarczyk, J., and Sojka, M.: Evaluation of Methods for Estimating Lake Surface Water Temperature Using Landsat 8, *Remote Sensing*, 14, 3839, <https://doi.org/10.3390/rs14153839>, 2022.
- Dye, A., Bryant, R., Doff, E., Falcini, F., and Rippin, D. M.: Warm Arctic Proglacial Lakes in the ASTER Surface Temperature Product, *Remote Sensing*, 13, 2987, <https://doi.org/10.3390/rs13152987>, 2021.
- 375 Earth Resources Observation and Science (EROS) Center: Landsat 8-9 Operational Land Imager / Thermal Infrared Sensor Level-2, Collection 2 [dataset], U.S. Geological Survey, <https://doi.org/10.5066/P9OGBGM6>, 2020.
- Feyisa, G. L., Meilby, H., Fensholt, R., and Proud, S. R.: Automated Water Extraction Index: A new technique for surface water mapping using Landsat imagery, *Remote Sensing of Environment*, 140, 23–35, <https://doi.org/10.1016/j.rse.2013.08.029>, 2014.
- 380 Gillies, S. et al.: Rasterio: geospatial raster I/O for Python programmers, Mapbox, <https://github.com/rasterio/rasterio>, 2013–.



- Goliber, S., Black, T., Catania, G., Lea, J. M., Olsen, H., Cheng, D., Bevan, S., Bjørk, A., Bunce, C., Brough, S., Carr, J., Cowton, T., Gardner, A., Fahrner, D., Hill, E., Joughin, I., Korsgaard, N. J., Luckman, A., Moon, T., Murray, T., Sole, A., Wood, M., , and Zhang, E.: TermPicks: a century of Greenland glacier terminus data for use in scientific and machine learning applications, *The Cryosphere*, 16, 3215–3233, <https://doi.org/10.5194/tc-16-3215-2022>, 2022.
- 385 Greenland Ecosystem Monitoring: BioBasis Nuuk - Lakes - Temperature in lakes (Version 1.0). [Data set] [CC-BY-SA-4.0], Greenland Ecosystem Monitoring, <https://doi.org/10.17897/BKTY-J070>, 2024.
- Grinsted, A., Hvidberg, C. S., Campos, N., and Dahl-Jensen, D.: Periodic outburst floods from an ice-dammed lake in East Greenland, *Scientific Reports*, 7, 9966, <https://doi.org/10.1038/s41598-017-07960-9>, 2017.
- Hansen, K., Karlsson, N. B., How, P., Poulsen, E., Mortensen, J., and Rysgaard, S.: Winter subglacial meltwater detected in Greenland Fjord, *Nature Geosciences*, In Press.
- 390 Holt, E., Nienow, P., and Medina-Lopez, E.: Terminus thinning drives recent acceleration of a Greenlandic lake-terminating outlet glacier, *Journal of Glaciology*, pp. 1–13, <https://doi.org/10.1017/jog.2024.30>, 2024.
- How, P.: PennyHow/GrIML v0.1.0, Zenodo, <https://doi.org/10.5281/zenodo.11395471>, 2024.
- How, P., Messerli, A., Mätzler, E., Santoro, M., Wiesmann, A., Caduff, R., Langley, K., Bojesen, M. H., Paul, F., Kääh, A., and Carrivick, J. L.: Greenland-wide inventory of ice marginal lakes using a multi-method approach, *Scientific Reports*, 11, 4481, <https://doi.org/10.1038/s41598-021-83509-1>, 2021.
- 395 How, P., Petersen, D., Karlsson, N. B., Kjeldsen, K. K., Raundrup, K., Messerli, A., Rutishauser, A., Carrivick, J. L., Lea, J. M., Fausto, R. S., Ahlstrøm, A. P., and Andersen, S. B.: Greenland Ice Marginal Lake Inventory annual time-series Edition 1 [dataset], GEUS Dataverse, <https://doi.org/10.22008/FK2/MBKW9N>, 2025.
- 400 Howat, I.: MEaSURES Greenland Ice Mapping Project (GIMP) land ice and ocean classification mask, version 1 [GimpIce-Mask 15 m tiles 0-5], NASA National Snow and Ice Data Center Distributed Active Archive Center, Boulder, Colorado USA, <https://doi.org/10.5067/B8X58MQBFUPA>, 2017.
- Howat, I. M., Negrete, A., and Smith, B. E.: The Greenland Ice Mapping Project (GIMP) land classification and surface elevation data sets, *Cryosphere*, 8, 1509–1518, <https://doi.org/10.5194/tc-8-1509-2014>, 2014.
- 405 Kelsey, J. et al.: geopandas/geopandas: v0.8.1, Zenodo, <https://doi.org/10.5281/zenodo.394676>, 2020.
- Kjeldsen, K. K., Mortensen, J., Bendtsen, J., Petersen, D., Lennert, K., and Rysgaard, S.: Ice-dammed lake drainage cools and raises surface salinities in a tidewater outlet glacier fjord, west Greenland, *Journal of Geophysical Research: Earth Surface*, 119, 1310–1321, <https://doi.org/10.1002/2013JF003034>, 2014.
- Kjeldsen, K. K., Khan, S. A., Bjørk, A. A., Nielsen, K., and Mougnot, J.: Ice-dammed lake drainage in west Greenland: Drainage pattern and implications on ice flow and bedrock motion, *Geophysical Research Letters*, 44, 7320–7327, <https://doi.org/10.1002/2017GL074081>, 2017.
- 410 Lutz, K., Bahrami, Z., and Braun, M.: Supraglacial Lake Evolution over Northeast Greenland Using Deep Learning Methods, *Remote Sensing*, 15, 4360, <https://doi.org/10.3390/rs15174360>, 2023.
- Lützwow, N., Veh, G., and Korup, O.: A global database of historic glacier lake outburst floods, *Earth System Science Data*, 15, 2983–3000, <https://doi.org/10.5194/essd-15-2983-2023>, 2023.
- 415 Malakar, N. K., Hulley, G. C., Hook, S. J., Laraby, K., Cook, M., and Schott, J. R.: An Operational Land Surface Temperature Product for Landsat Thermal Data: Methodology and Validation, *IEEE Transactions on Geoscience and Remote Sensing*, 56, 5717–5735, <https://doi.org/10.1109/TGRS.2018.2824828>, 2018.



- Mallalieu, J., Carrivick, J. L., Quincey, D. J., and Raby, C. L.: Ice-marginal lakes associated with enhanced recession of the Greenland Ice Sheet, *Global and Planetary Change*, 202, 103–503, <https://doi.org/10.1016/j.gloplacha.2021.103503>, 2021.
- McFeeters, S. K.: The use of the Normalized Difference Water Index (NDWI) in the delineation of open water features, *International Journal of Remote Sensing*, 17, 1425–1432, <https://doi.org/10.1080/01431169608948714>, 1996.
- Melling, L., Leeson, A., McMillan, M., Maddalena, J., Bowling, J., Glen, E., Sandberg Sørensen, L., Winstrup, M., and Lørup Arildsen, R.: Evaluation of satellite methods for estimating supraglacial lake depth in southwest Greenland, *The Cryosphere*, 18, 543–558, <https://doi.org/10.5194/tc-18-543-2024>, 2024.
- Moon, T. A., Fisher, M., Stafford, T., and Thurber, A.: QGreenland (v3), National Snow and Ice Data Center, <https://doi.org/10.5281/zenodo.12823307>, 2023.
- Mouginot, J. and Rignot, E.: Glacier catchments/basins for the Greenland Ice Sheet, Dryad, <https://doi.org/10.7280/D1WT11>, 2019.
- Naalakkersuisut: Impact Analysis of the Paris Agreement on Greenlandic Society, https://naalakkersuisut.gl/-/media/horinger/2023/02/0602_parisaftale/eng-hovedrapport--konsekvensanalyse-af-parisaftalen-for-det-grnlandske-samfund.pdf, accessed: 2024-11-01, 2023.
- NASA Applied Remote Sensing Training (ARSET) program: ARSET Training: Satellite Remote Sensing for Measuring Urban Heat Islands and Constructing Heat Vulnerability Indices, <https://code.earthengine.google.com/7103291d8b113cd38e573f2e3a67bb51>, accessed: 2024-12-02, 2022.
- Ran, J., Ditmar, P., van den Broeke, M. R., Liu, L., Klees, R., Khan, S. A., Moon, T., Li, J., Bevis, M., Zhong, M., Fettweis, X., Liu, J., Noël, B., Shum, C. K., Chen, J., Jiang, L., and van Dam, T.: Vertical bedrock shifts reveal summer water storage in Greenland ice sheet, *Nature*, 635, 108–113, <https://doi.org/10.1038/s41586-024-08096-3>, 2024.
- Rick, B., McGrath, D., Armstrong, W., and McCoy, S. W.: Dam type and lake location characterize ice-marginal lake area change in Alaska and NW Canada between 1984 and 2019, *The Cryosphere*, 16, 297–314, <https://doi.org/10.5194/tc-16-297-2022>, 2022.
- Rick, B., McGrath, D., McCoy, S. W., and Armstrong, W. H.: Unchanged frequency and decreasing magnitude of outbursts from ice-dammed lakes in Alaska, *Nature Communications*, 14, 6138, <https://doi.org/10.1038/s41467-023-41794-6>, 2023.
- Shugar, D. H., Burr, A., Haritashya, U. K., Kargel, J. S., Watson, C. S., Kennedy, M. C., Bevington, A. R., Betts, R. A., Harrison, S., and Strattman, K.: Rapid worldwide growth of glacial lakes since 1990, *Nature Climate Change*, 10, 939–945, <https://doi.org/10.1038/s41558-020-0855-4>, 2020.
- Styrelsen for Dataforsyning og Infrastruktur: Sentinel2 10m 2022 mosaic. In: *Satellitfoto Grønland*, <https://dataforsyningen.dk/data/4783>, accessed: 2024-12-02, 2024.
- Sutherland, J. L., Carrivick, J. L., Gandy, N., Shulmeister, J., Quincey, D. J., and Cornford, S. L.: Proglacial Lakes Control Glacier Geometry and Behavior During Recession, *Geophysical Research Letters*, 47, e2020GL088865, <https://doi.org/10.1029/2020GL088865>, 2020.
- Tomczyk, A. M., Ewertowski, M. W., and Carrivick, J. L.: Geomorphological impacts of a glacier lake outburst flood in the high arctic Zackenberg River, NE Greenland, *Journal of Hydrology*, 591, 125–300, <https://doi.org/10.1016/j.jhydrol.2020.125300>, 2020.
- Veh, G., Lützw, N., Tamm, J., Luna, L. V., Hugonnet, R., Vogel, K., Geertsema, M., Clague, J. J., and Korup, O.: Less extreme and earlier outbursts of ice-dammed lakes since 1900, *Nature*, 614, 701–707, <https://doi.org/10.1038/s41586-022-05642-9>, 2023.
- Wieczorek, I., Strzelecki, M. C., Stachnik, Ł., Yde, J. C., and Małeck, J.: Post-Little Ice Age glacial lake evolution in Svalbard: inventory of lake changes and lake types, *Journal of Glaciology*, 69, 1449–1465, <https://doi.org/10.1017/jog.2023.34>, 2023.
- Wiesmann, A., Santoro, M., Caduff, R., How, P., Messerli, A., Mätzler, E., Langley, K., Høegh Bojesen, M., Paul, F., and Kääh, A. M.: ESA Glaciers Climate Change Initiative (Glaciers_cci): 2017 inventory of ice marginal lakes in Greenland (IIML), v1, Centre for Environmental Data Analysis, <https://doi.org/10.5285/7ea7540135f441369716ef867d217519>, 2021.



- Wilkinson, M. D., Dumontier, M., Aalbersberg, I. J., Appleton, G., Axton, M., Baak, A., Blomberg, N., Boiten, J.-W., da Silva Santos, L. B., Bourne, P. E., Bouwman, J., Brookes, A. J., Clark, T., Crosas, M., Dillo, I., Dumon, O., Edmunds, S., Evelo, C. T., Finkers, R., Gonzalez-Beltran, A., Gray, A. J., Groth, P., Goble, C., Grethe, J. S., Heringa, J., 't Hoen, P. A., Hooft, R., Kuhn, T., Kok, R., Kok, J., Lusher, S. J., Martone, M. E., Mons, A., Packer, A. L., Persson, B., Rocca-Serra, P., Roos, M., van Schaik, R., Sansone, S.-A., Schultes, E., Sengstag, T., Slater, T., Strawn, G., Swertz, M. A., Thompson, M., van der Lei, J., van Mulligen, E., Velterop, J., Waagmeester, A., Wittenburg, P., Wolstencroft, K., Zhao, J., and Mons, B.: The FAIR Guiding Principles for scientific data management and stewardship, *Scientific Data*, 3, 2052–4463, <https://doi.org/10.1038/sdata.2016.18>, 2016.
- 460
- Winstrup, M., Ranndal, H., Hillerup Larsen, S., Simonsen, S. B., Mankoff, K. D., Fausto, R. S., and Sandberg Sørensen, L.: PRODEM: an annual series of summer DEMs (2019 through 2022) of the marginal areas of the Greenland Ice Sheet, *Earth System Science Data*, 16, 5405–5428, <https://doi.org/10.5194/essd-16-5405-2024>, 2024.
- 465
- Xu, H.: Modification of normalised difference water index (NDWI) to enhance open water features in remotely sensed imagery, *International Journal of Remote Sensing*, 27, 3025–3033, <https://doi.org/10.1080/01431160600589179>, 2006.
- Zhang, E., Catania, G., and Trugman, D. T.: AutoTerm: an automated pipeline for glacier terminus extraction using machine learning and a “big data” repository of Greenland glacier termini, *The Cryosphere*, 17, 3485–3503, <https://doi.org/10.5194/tc-17-3485-2023>, 2023a.
- 470
- Zhang, G., Bolch, T., Yao, T., Rounce, D., Chen, W., Veh, G., King, O., Allen, S. K., Wang, M., and Wang, W.: Underestimated mass loss from lake-terminating glaciers in the greater Himalaya, *Nature Geoscience*, 16, 333–338, <https://doi.org/10.1038/s41561-023-01150-1>, 2023b.
- Zhang, G., Carrivick, J. L., Emmer, A., Shugar, D. H., Veh, G., Wang, X., Labedz, C., Mergili, M., Mølg, N., Huss, M., Allen, S., Sugiyama, S., and Lützw, N.: Characteristics and changes of glacial lakes and outburst floods, *Nature Reviews Earth and Environment*, 5, 447–462, <https://doi.org/10.1038/s43017-024-00554-w>, 2024.
- 475

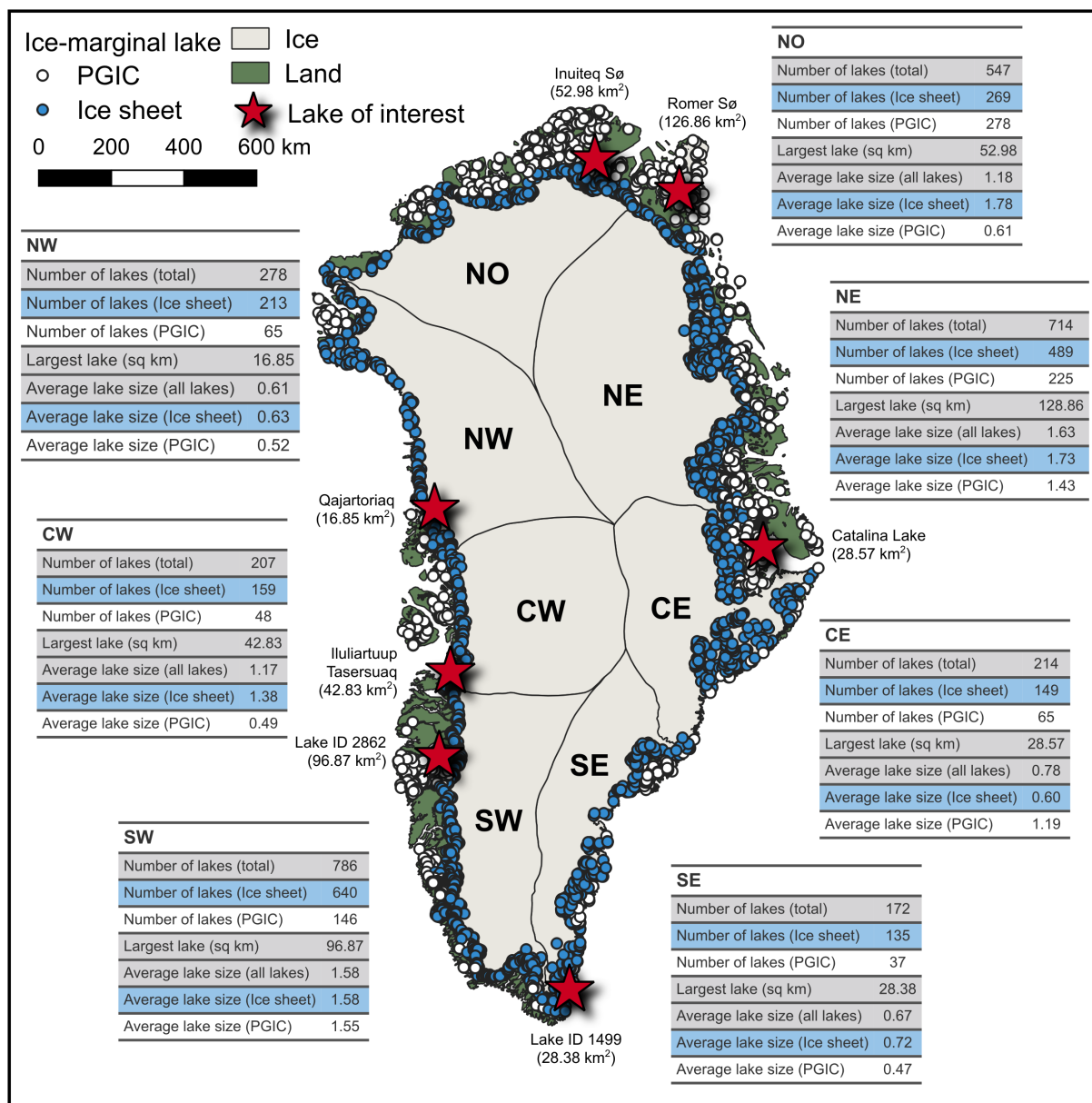


Figure 1. An overview of the abundance of lakes in ice-marginal lake inventory series, 2016-2023. Each mapped point denotes a unique lake, mapped across the Greenland Ice Sheet margin (blue) and the surrounding PGIC margins (white). The tables associated with each region present general statistics, with red starred points on the map corresponding to the largest lake of each region. Placenames for the largest lakes are sourced from the placename database provided by Oqaasileriffik (the Language Secretariat of Greenland), with inventory identification numbers presented where a name is not given. It is noted that the name of the largest lake in the CE region (Catalina Lake) is not present in the placename database, and instead we adopt the lake name from Grinsted et al. (2017). The catchment regions are those defined by Mouginot and Rignot (2019). Base maps for plotting are from QGreenland v3.0 (Moon et al., 2023).

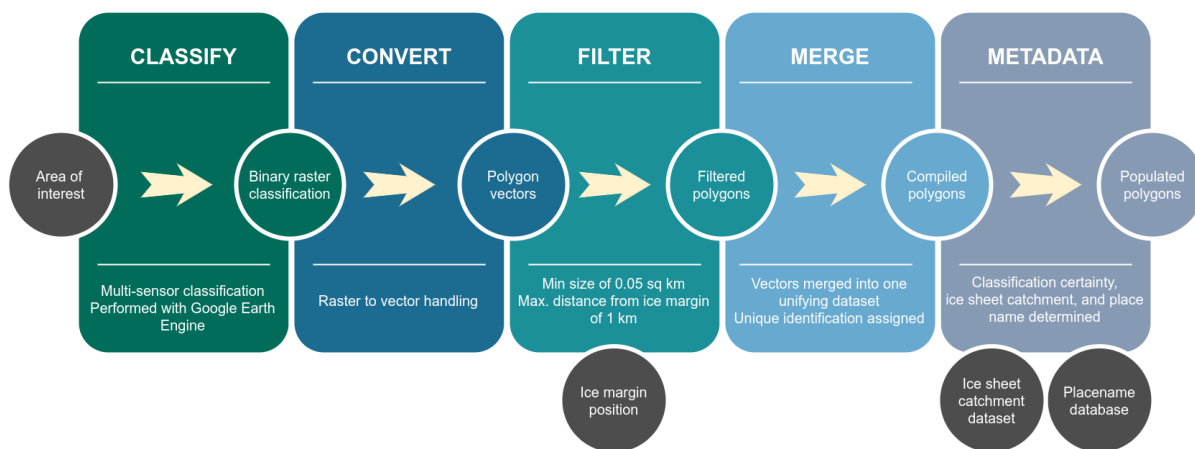


Figure 2. A visualisation of the processing workflow for the generation of the ice-marginal lake inventory series, including components performed with © Google Earth Engine ("Classify") and the Python package GrIML (How, 2024), which utilises Python spatial data handling packages geopandas (Kelsey et al., 2020) and rasterio (Gillies et al., 2013–). The workflow is based on How et al. (2021). The annotated rectangles refer to process stages (reading from left to right), the coloured annotated circles represent intermediary outputs to the corresponding process stages in the workflow, and the grey annotated circles represent workflow inputs.

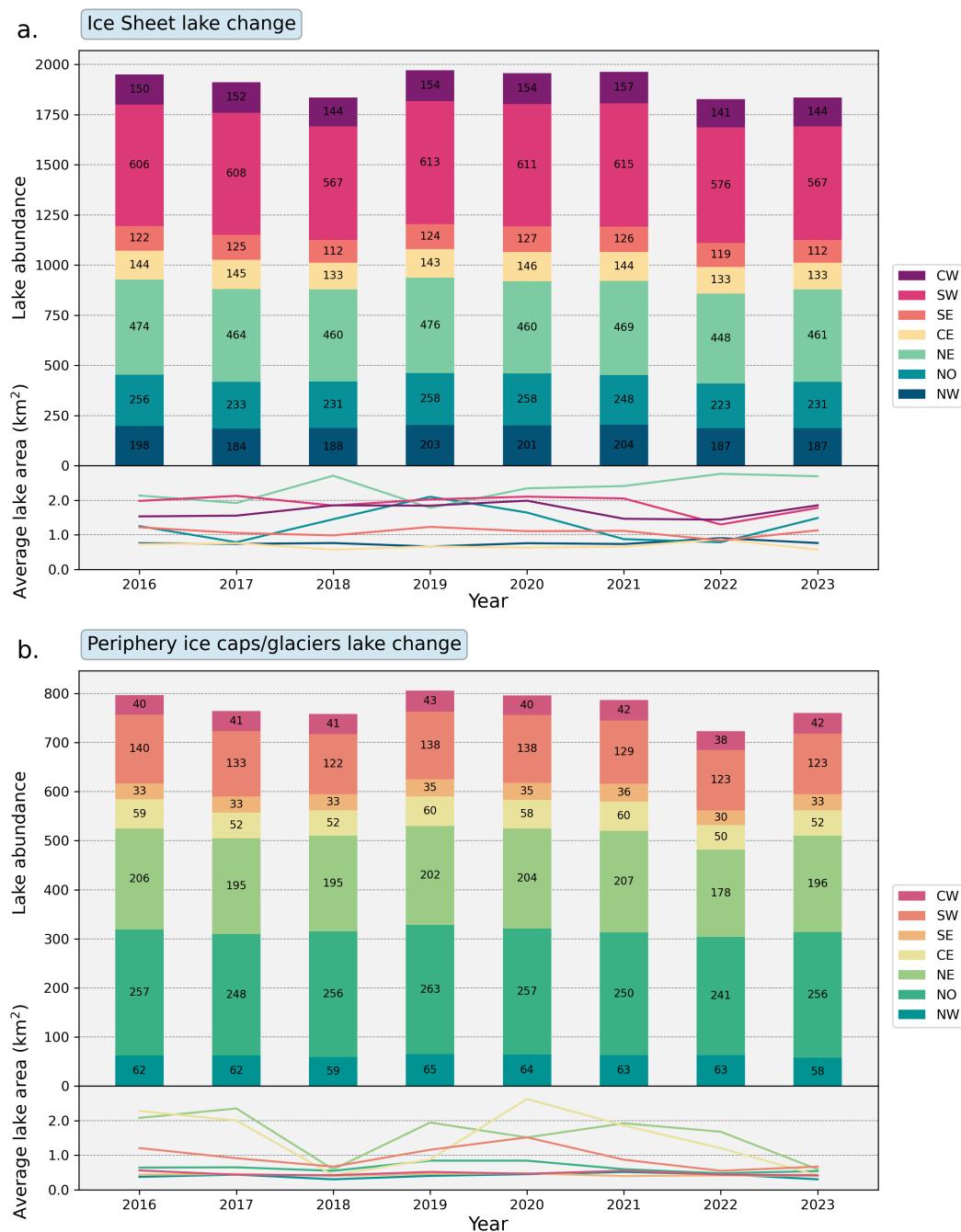


Figure 3. Change in the abundance and average area (km^2) of ice-marginal lakes around the ice sheet margin (a) and PGIC margins (b). Each of the coloured bars denote lake abundance per region for a given year of the inventory series (2016-2023), with annotated numbers corresponding to the number of lakes classified for each region. Each line plot indicates the average lake area per region for a given year of the inventory series. Average lake area is compiled from all lakes classified from SAR and multi-spectral imagery, as DEM classifications are not a direct detection of water bodies.

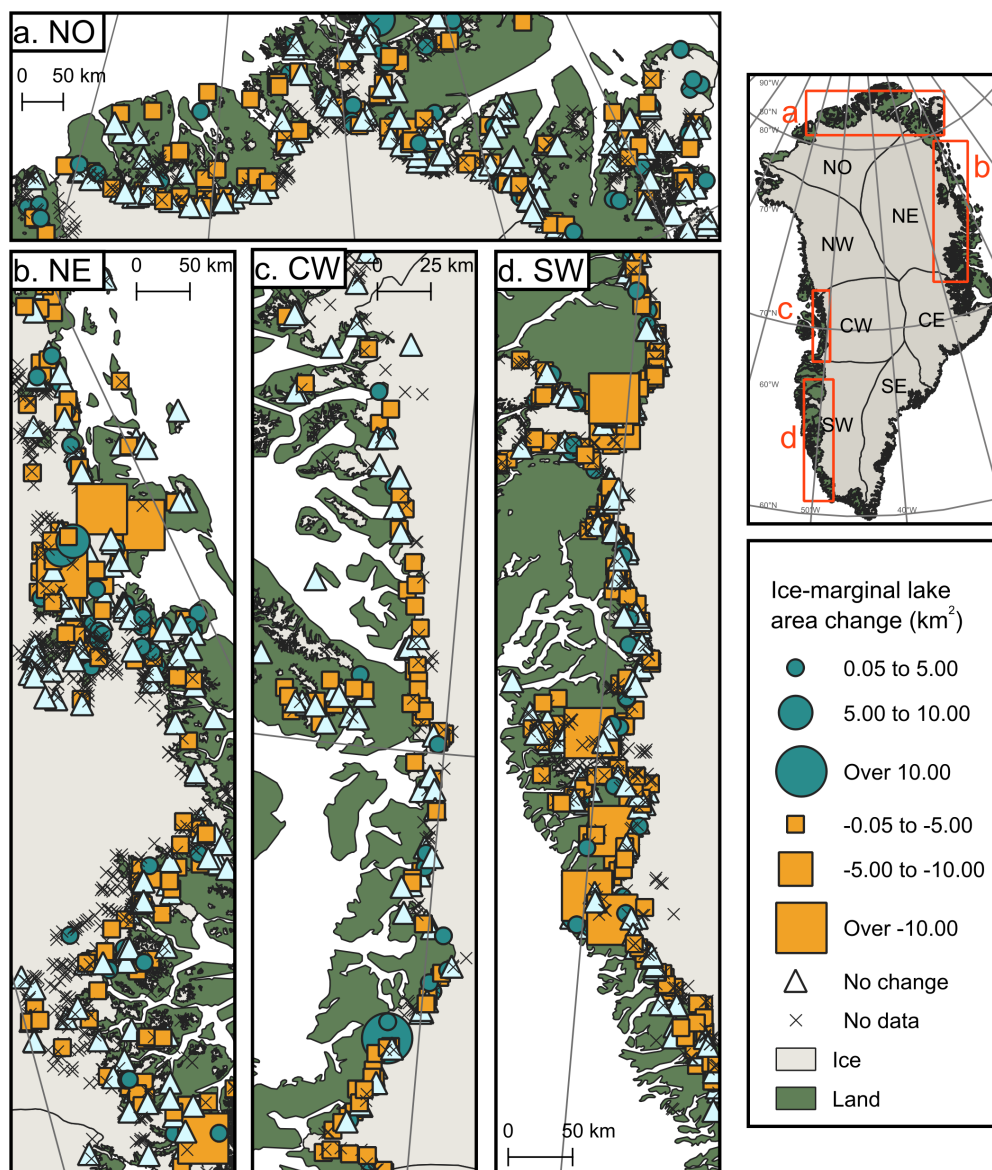


Figure 4. Change in lake area across the ice-marginal lake inventory series, 2016-2023. Example regions are highlighted from NO (a), NE (b), CW (c), and SW (d) regions of both the ice sheet and the PGICs. Lake area increase (purple circles), lake area decrease (yellow squares), and unchanged lake areas (white triangles) are mapped, with the size of the symbol denoting the amplitude of change (km^2). Each point denotes the change in lake size across the inventory series, as classified using the SAR and multi-spectral imagery methods. Lakes with no available area data (i.e. not classified using the SAR and multi-spectral imagery methods) are marked with crosshairs. The catchment regions are those defined by Mouginot and Rignot (2019). Base maps for plotting are from QGreenland v3.0 (Moon et al., 2023).

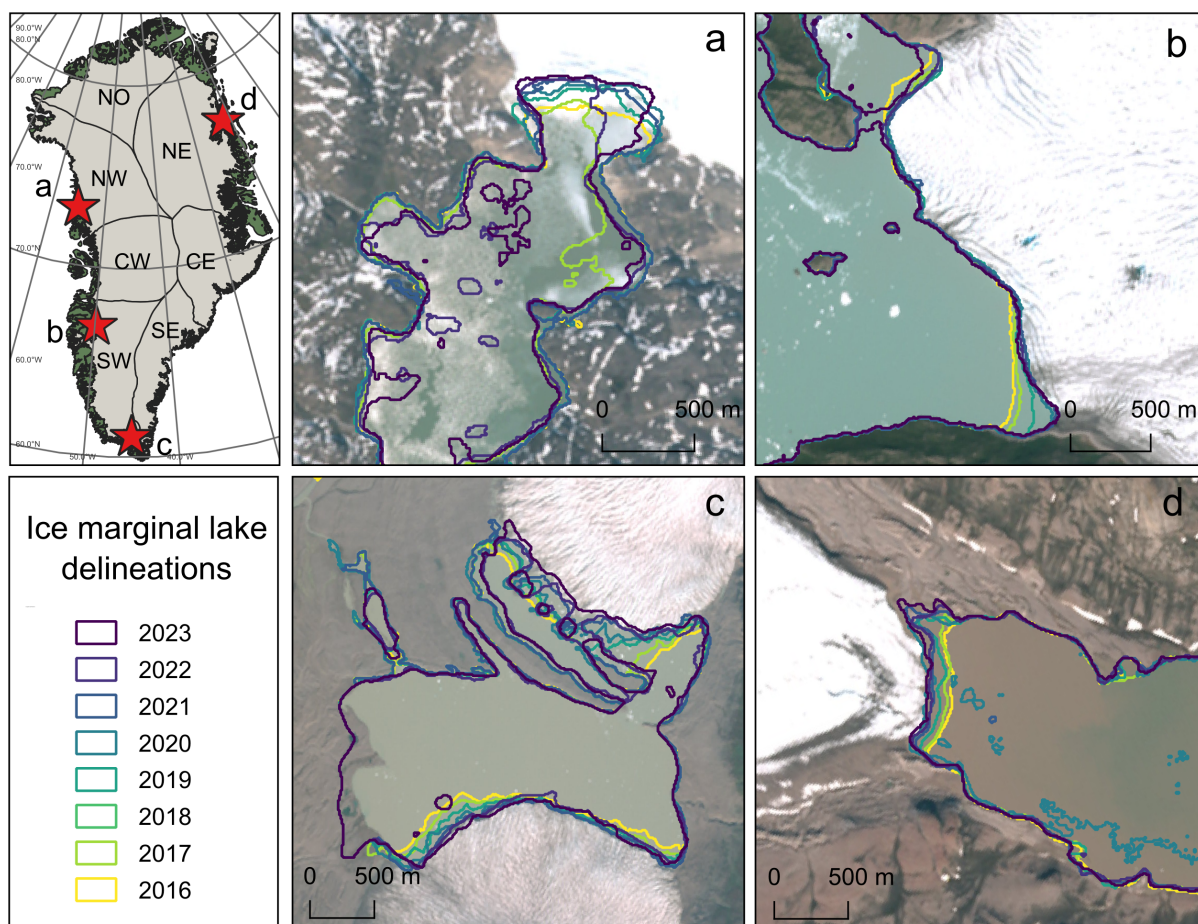


Figure 5. Examples of lake morphology change, and the corresponding evolution of ice termini morphology, from the ice-marginal lake inventory series. These examples highlight basin margin retreat (a), peripheral margin retreat (b), bilateral margin retreat (c), and focused margin retreat (d). The background satellite imagery presented is from a Sentinel-2 10 m 2022 mosaic (Styrelsen for Dataforsyning og Infrastruktur, 2024). The base layers for the insert map plotting are from QGreenland v3.0 (Moon et al., 2023).

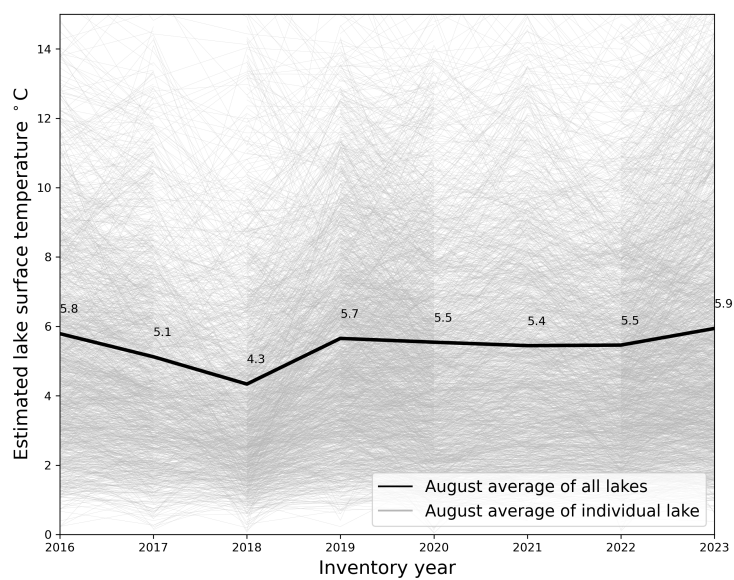
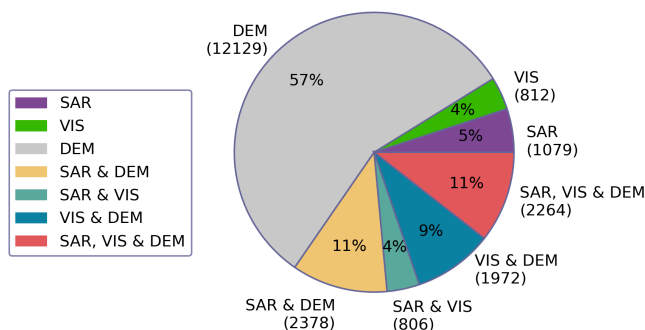


Figure 6. Average surface lake temperature estimates from the month of August at each inventory lake for each inventory year (2016-2023) (grey), with the average of all lakes overlaid (black). Surface lake temperature is derived from Landsat 8 and Landsat 9 OLI/TIRS Collection 2 Level 2 surface temperature data product. Averages are calculated from all available scenes acquired from the month of August to limit the risk of mis-estimates due to ice-covered conditions.



a. Methodology performance for lake detection across all inventory years (2016-2023)



b. Ice sheet by region

c. PGIC by region

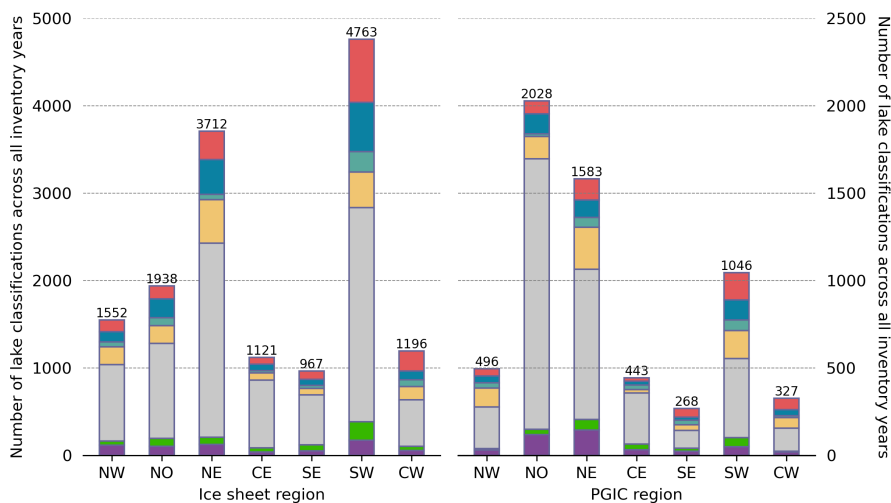


Figure 7. Lake classifications by method across the ice-marginal lake inventory series, with an overview of lake classifications over all inventory years (a) and classifications by region for lakes adjacent to the ice sheet (b) and the PGICs (c). SAR refers to the SAR backscatter classification method from Sentinel-1 imagery, VIS refers to the multi-spectral classification method from Sentinel-2 imagery, DEM refers to the DEM sink detection method from the ArcticDEM, and listed methods refer to instances where more than one method has been used to classify a lake (e.g. "SAR & DEM", "SAR, VIS & DEM"). The legend and colour scheme in (a) correspond to (b) and (c). Values in brackets in (a) are the absolute number of lakes corresponding to the provided percentages. The values printed on top of the bars in (b) are the total number of classifications in the given region.

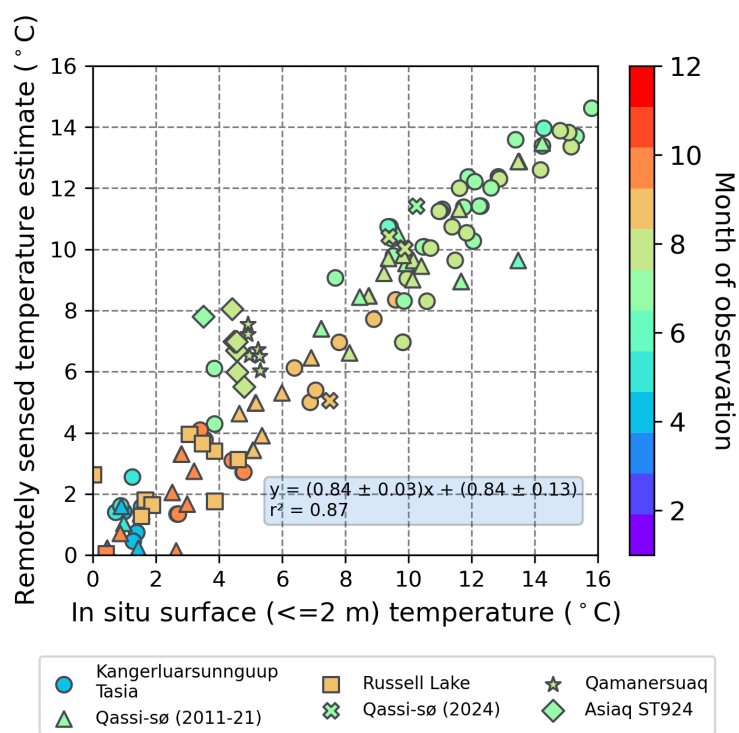


Figure 8. Comparison of in situ surface (<= 2 m) water temperature measurements with remotely sensed temperature estimates (°C) from Kangerluarsunnguup Tasia (circle), Qassi-Sø (2011-21) (triangle), Russell Lake (square), Qassi-Sø (2024) (cross), Qamanersuaq (star) and Asiaq station 924 (ST924) (diamond). The colour of each point corresponds to the month that the observation was collected.